附件一

出國報告（出國類別：出席會議）

參加 2012 IEEE 國際諧波與電力品質會議（2012 IEEE International Conference on Harmonics and Quality of Power）

服務機關：國立中正大學

姓名職稱：張文恭　教授、蘇懷哲 學生、盧恆究 學生

派赴國家：香港

出國期間：101 年 6 月 17 日至 101 年 6 月 21 日

報告日期：101 年 7 月 2 日

摘 要

2012 年第 15 屆 IEEE 國際諧波與電力品質研討會議 (International Conference on Harmonics and Quality of Power – ICHQP，前身為電力系統諧波國際會議 - ICHPS)於 6 月 17 至 20 日於香港舉辦，為針對現今與未來國際上電力諧波與電力品質發展趨勢之主要會議。會議主軸為邀請世界各國從事電力諧波與電力品質相關研究之學者參加，並進行相關議題之討論與報告。會議期間計有二十二場分組專題會議與四場特別專題報告。

此次出國目的在於參與每二年舉行一次之 IEEE 國際諧波與電力品質會議，本人除了擔任本大會之國際議程推動委員外，亦在本會議規劃一場全體會議(Plenary Session)及擔任主持人，同時進行一場相關研究論文之發表。本次行程同時帶領二名博士生盧恆究與蘇懷哲參與學術論文發表，並在會議最後一日參訪香港電燈電力公司。

目　次

壹、目的

2012 年 IEEE 國際電力品質與諧波會議於 6 月 17 至 20 日共 4 天，於中國香港舉行。本次會議由香港理工大學主辦，香港電力公司協辦，另有十餘家香港或國際廠商贊助。主辦單位邀請了二十餘國學者與業界人士參加，除了增進相關實務經驗外亦可瞭解當代電力品質技術與理論。此次出國目的在於參與每二年舉行一次之國際諧波與電力品質會議，本人除了擔任 International Steering Committee 委員外，亦規劃一場全體會議。另外，帶領二名博士生同行，並發表三篇論文。

貳、過程

2012 年 IEEE 國際諧波與電力品質會議（2012 IEEE ICHQP）於香港舉行，會議時間自 6 月 17 日至 6 月 20 日共 4 日。該會議為少數重要之國際電力品質學術會議，論文接受率約 55%，本次會議計有 180 餘篇論文發表於 16 個不同之論文及全體會議，另有二場參訪香港中電之行程，與會者逾 400 人。本次會議主要場地位於九龍香格里拉大旅館舉行，本人規劃與主持之全體會議 2 於 6 月 18 日下午 3 時進行，除了發表論文之外，亦與逾 80 位之學業界人士進行深入之討論與交流。此外，本人亦參與 6 月 18 日至 6 月 20 日多場之論文發表與 Keynote Speech。

本次行程同時帶領二名博士生盧恆究與蘇懷哲參與學術論文發表，並在會議最後一日參訪香港電燈電力公司。本次行程計四日，扣除往返機程及報到日(101 年 6 月 17 日)，其他行程如下：

第一天(101 年 6 月 17 日)：去程及參與大會歡迎晚宴

第二天(101 年 6 月 18 日)：參與開幕專題演講

參與 Plenary Session 1：電力品質干擾訊息萃取(Information Extraction from PQ Disturbances)

主持 Plenary Session 2：智慧電網技術之電力品質管理(Smart Grid Technologies for PQ Management)

論文發表：對於智慧電網之電力品質方面的監測問題與分析技術 (Monitoring Issues and Analysis Techniques-Smart Grid Aspect of Power Quality)

第三天(101 年 6 月 19 日)：

參與 Plenary Session 3：目前電力品質監測之實行與未來挑戰 (Current Practice and Future Challenges for PQ Monitoring)

參與論文發表會：電力品質擾動緩解全系統之解決方案 (system-wide Solutions for PQ Disturbance

Mitigation)

第四天(101 年 6 月 20 日)：

發表論文 (1) 應用灰色模型預測電弧爐閃爍嚴重性 (Application of Grey Predictor Model for Forecasting Flicker Severity Associated with Electric Arc Furnaces)，如附件一所示。

(2) 靜態無效功率補償器裝置於變電站網路中的電壓閃爍緩解措 (Feasibility Study of SVC Installation in A Substation Network for Voltage Fluctuation Mitigation)，如附件一所示。

(3) 諧波研究之交流微網建模與模擬 (Modeling and Simulation of an AC Microgrid for Harmonics Study)，如附件一所示。

發表論文題目	報告內容重點摘述與發表文章簡述	發表文章交流內容簡述
應用灰色模型預測電弧爐閃爍嚴重性	由於電弧爐負載引起快速的電壓波動可能會產生電壓閃爍現象，而負面影響到人的眼睛和電力系統元件。本文提出了灰色模型預測電弧爐負載之電壓閃爍嚴重程度。採用實測數據，以實現預測模型。基於該模型的試驗結果與其他兩個神經網絡方法進行比較。而且由結果表示，本文提出之方法實現電壓閃爍嚴重程度預測更為準確。	會議中，由相關學者提出本論文之疑問： 1.實測資料圖形呈現是否已經透過灰色理論之累加生成後表現。 2.如何將灰色模型中的參數有效完整應用於本文問題，以得到更精確之結果。
靜態無效功率補償器裝置於變電站網路中的電壓閃爍緩解措施之可行性研究	在電力系統互聯下，具有隨機與激烈電壓電流特性的電弧爐運轉產生可觀的電力品質問題。由於電弧爐負載在運轉期間的非線性特性，在連接的匯流排上可觀測到嚴重電壓擾動，而且會造成有載分接頭頻繁的動作，此會造成減短有載分接頭壽命與影響電力品質，因此實行相關抑制策略是必要的。本文探討在供電給兩個大型電弧爐負載真實變電所系統中安裝 SVC 之可行性作為抑制減輕電壓變動與有載分接頭動作次數。	會議中，由相關學者提出本論文之疑問： 1.如何找出主要電壓變動來源方法，以及系統建模方法。
諧波研究之交流微網建模與模擬	發展含有分散式發電之微電網能夠減低建設石化燃料為基礎的電廠成本與碳排放、提供無效功率補償與頻率調節	會議中，由相關學者提出本論文之疑問：

	功能、增加備轉容量與增強系統穩定度。然而分散式發電與非線性負載運轉將會伴隨著像不平衡、電壓變動與諧波等負面影響，這會影響微電網系統的電力品質。本文章將探討交流微電網中的諧波衝擊模擬研究與抑制方法的成效。而模擬結果將指出潛在諧波問題，以及顯示諧波抑制策略對於微電網規劃之可行性。	1.非線性負載與分散式發電建立等效模型方法如何實現。 2.改善設備之安裝位置與參數考量與設計方法。

下午參訪香港電燈電力公司之市區變電所與電力品質用戶展示中心。

第五天(101 年 6 月 21 日)：返程

本人在主持之全體會議 2 亦發表一篇論文，主要在於探討智慧電網發展過程中應重視之電力品質分析與技術議題。另有上列三篇文章由學生發表，則著重於微電網之電力諧波分析，電力系統之閃爍預測及抑制方法之可行性評估。

參、心得

電力品質與智慧電網發展之一環，藉由電力品質之提升與資通訊之技術結合，及即時監控技術之整合與輸配電系統之供電品質與大幅提升，並減少輸電損失，增進系統之可靠度。電力品質之發展為智慧監控、再生能源、與資通訊技術之整合，對智慧電網的發展有很重要的影響。

電力品質為先進國家重視之用電指標，在智慧電網發展之同時，電力品質之提升亦為各先進國家重視。藉由本次會議之參與，本人與不同國家之專家學者交流，提升相關領域之視野，並瞭解最近二年電力品質方面之研究與發展。

肆、建議

1. 與智慧電網相關之電力品質技術近年受到相當重視，在電力系統之發展上可加強研究與落實相關技術發展。
2. 智慧電網相關之電力品質技術在可預見的未來，佔比將逐漸增加，對再生能源普及有重要影響。
3. 電力品質之優劣為評量國家供電可靠度之重要指標，在相關之規範與技術提升可多參與國際合作。
4. 雲端技術發展，亦可用於電力品質資料庫方面之應用。
5. 電力品質議題不僅於對高科技產業重要，對於一般重工業、青工業甚至民生都有相當影響，而諧波與電力品質國際研討會可提供對於各國實務上如何克服相關電力品質問題的寶貴經驗，已提升我國電力品質層級。
6. 現今能源之應用議題，無論石化能源的枯竭或是新能源的開發，皆離不開電力品質和

能源轉換之間的效能提升關係，藉由分析供電品質，減少其電力轉換損失，即可達到節能之目的，此為密不可分之相輔關係，討論由電力系統中經常發生之異常電力品質現象問題。

伍、攜回資料名稱及內容

會議論文電子檔隨身碟。

陸、香港電燈電力公司參訪照片及論文海報

(1) 目的：本次藉由 2012 年 IEEE 國際諧波與電力品質會議之技術參訪香港電燈有限公司，由於全球因應節能減碳趨勢，各國積極投入相關應用，即是希望經由實地察訪與面談，試著了解香港電燈電力公司，是否有藉著數位電表的全面建置，進行多角化的規劃，因全球趨勢更會進一步衍生電力品質相關問題，並對其電力技術商業化之推動與營運，深入研習，以供台灣電業未來之規劃、開發、推動相關事業之參考。

(2) 內容：技術參訪為 2012 年 IEEE 國際諧波與電力品質會議之第四天(101 年 6 月 20 日)下午兩點到下午五點半時段，共約 3.5 小時，其中了解香港電燈電力公司為電能實業於香港之主要營運公司，創立於一八八九年，是為目前世界上歷史最悠久電力公司之一。經由前述針對香港電燈有限公司過去之基本簡介後，接著參觀該公司對於未來再生能源應變政策與安裝再生能源機組之架設以及針對電力品質之要求與改善措施與電力系統技術維護說明，如附件二所示。

(3) 見聞與效益：全球因應節能減碳趨勢，各國積極投入相關應用，智慧電網成為目前國際間熱門議題，而智慧電表為其重要組成，其可提供資訊使消費者聰明用電，在搭配有效的時間電價後，更可能平滑尖峰負載，使電力供應者可以經濟產電，智慧電網統另一項重要的特性，是其有能力應付發電資源更為分散之網路，包括可將電力回售給電網之分散型電源，例如住家之太陽能面板及插電式油電混合車，並可進而提供附加服務，而以上趨勢更會進一步衍生電力品質相關問題與發展多角化事業，提升台灣電業專業技術水平。

附件一

Paper 31

Application Of Grey Predictor Model For Forecasting Flicker Severity Associated With Electric Arc Furnace Load

2012 IEEE International Conference on Harmonics and Quality of Power

Application of Grey Predictor Model for Forecasting Flicker Severity Associated with Electric Arc Furnace Load

G. W. Chang, *Fellow, IEEE*, H. J. Liu, and H. J. Su
Department of Electrical Engineering, Chang Cheng University
Chiayi, TAIWAN, R.O.C.

Abstract

It is known that rapid voltage fluctuations caused by electric arc furnace loads may generate significant levels of flicker, which have negative impacts to human eyes and power system components. This paper proposes a grey predictor model for the forecast of flicker levels produced by an electric arc furnace load. Actual measured data are adopted to implement the predictor model. Test results based on the proposed model are compared with two other neural network methods. It shows that more accurate forecast is achieved for the flicker prediction based on the proposed method.

***Index Terms*— Grey theory, flicker, electric arc furnace, forecast.**

I. Introduction

Voltage fluctuations produced by fluctuating loads in the power system may lead to undesirable illumination flickers of lighting [1]. Therefore, an accurate model for flicker level is needed. In general, the flicker types may fall into two categories: cyclic and aperiodic. Flicker is a repetitive one and is caused by periodic voltage fluctuations due to the operation of loads such as spot welders, compressors, or arc furnaces. Nonperiodic flicker is produced by irregular fluctuations, such as starting large motors. Some types of loads such as arc furnaces may produce both cyclic and nonperiodic flickers.

In the literature, grey forecasting models have been widely used in different applications [12]-[15]. This paper presents the forecast of flicker level produced by an electric arc furnace (EAF) based on adopting the first-order one-variable model GM(1,1) in the proposed model, the raw data of measured flicker are through accumulated generating operations. Then, the grey modeling and the inverse accumulated generating operation are performed. Results obtained by the forecasting model are compared with two other commonly used methods, back-propagation neural network (BPNN) and radial basis function neural network (RBFNN) [16]-[17]. It shows that more accurate results are obtained for flicker forecasting based on the proposed grey model.

II. Flicker Measurement

The voltage including flicker components can be expressed by the amplitude modulated (AM) signal of [1]:

$$v(t) = \left[A_1 + \sum_{k=1} A_k \cos(\omega_k t + \phi_k)\right]\cos(\omega_0 t + \phi_0) \tag{1}$$

where $A(t)$ is the amplitude of the nominal power system voltage, $\omega_0 t$ is the nominal power frequency, and ϕ_0 is the nominal phase angle. Furthermore, A_k is the amplitude of the kth flicker voltage; ω_k and ϕ_k are its associated frequency and phase angle, respectively; m is the number of flicker components.

Other than the commonly used flicker indices of short-term flicker severity (P_{ST}) and long-term flicker severity (P_{LT}) in North America and Europe, the flicker severity index, equivalent 10-Hz voltage flicker, ΔV_{10}, developed by the Central Research Institute of the Electric Power Industry (CRIEPI) of Japan has been adopted to some Asian countries for over two decades [18]. The voltage flicker at 10-Hz equivalent value, ΔV_{10}, is defined as the flicker severity level and is given by (2):

$$\Delta V_{10} = \sqrt{\sum_k k \cdot \Delta V_{ak}^2} \tag{2}$$

where ΔV_{ak} represents the fluctuation amplitude of the specified n-th frequency component and k is the equivalent sensitivity coefficient of the corresponding component with respect to 10-Hz, as shown in Fig. 1, which describes the sensitivity of human eye from incandescent or fluorescent flicker. For a 100V and 50-Hz system, the flicker will be perceptible (i.e. 1 pu) as $\Delta V10$ is 0.45 V at 10 Hz [18]. Therefore, 0.45% is set as the limit for the flicker severity.

Fig. 1. Sensitivity coefficient curve for $\Delta V10$ measurement.

III. Grey Model GM(1,1)

A grey model is often used to forecast future values of a time series according to the most recent data set [11]. The grey system theory performs the estimation of practical processing laws of the system based on the available data. In grey system theory, GM(*n*,*r*) is defined as a grey model, where *n* is the order of the reference equation and *r* is the number of variables. The GM(1,1) is the most commonly used grey model and is a time-series forecasting model which comprises a group of differential equations with time-varying coefficients. GM(1,1) model is only applied to positive data sequences. Though it is not necessary to employ all the data from the original series to construct GM(1,1), the data must be taken at equal intervals and in consecutive order without neglecting any data. Provided with input data series, major steps of applying GM(1,1) model for the output forecast are listed below.

Step 1: Create the original data series, $x^{(0)}$:

$$x^{(0)} = \{x^{(0)}(1), x^{(0)}(2), x^{(0)}(3), \ldots, x^{(0)}(n)\} \tag{3}$$

where n is the number of measured data obtained and $n \geq 4$.

Step 2: A new data set $x^{(1)}$ is generated by the accumulated generating operation (AGO) applied to the original data set $x^{(0)}$:

$$x^{(1)} = \{x^{(1)}(1), x^{(1)}(2), x^{(1)}(3), \ldots, x^{(1)}(n)\} \tag{4}$$

where

$$x^{(1)}(k) = \sum_{i=1}^{k} x^{(0)}(i), \quad k = 1, 2, \ldots, n \tag{5}$$

Define the generated mean sequence $z(1)$ of $x(1)$ as

$$z^{(1)} = \{z^{(1)}(2), z^{(1)}(3), z^{(1)}(4), \ldots, z^{(1)}(n)\} \tag{6}$$

where

$$z^{(1)}(k) = \{x^{(1)}(k) + x^{(1)}(k-1)\}/2, \quad k = 1, 2, \ldots, n-1 \tag{7}$$

Then, the least square forecast sequence of the grey difference equation for GM(1,1) is defined as (8) and the whitening equation is given by (9) at next step.

$$x^{(0)}(k) + az^{(1)}(k) = u \tag{8}$$

Step 3: Establishing the first-order differential equation for $x^{(1)}(k)$:

$$\frac{dx^{(1)}(k)}{dt} + ax^{(1)}(k) = u \tag{9}$$

where a and u denote two parameters.

Step 4: Calculating the parameters a and u of the differential equation in Step 3

$$\hat{B} = [a \quad u] = (B^T B)^{-1} B^T Y \tag{10}$$

where

$$B = \begin{bmatrix} -z^{(1)}(2) & 1 \\ -z^{(1)}(3) & 1 \\ \vdots & \vdots \\ -z^{(1)}(n) & 1 \end{bmatrix} \tag{11}$$

$$Y = [x(0)(2), x(0)(3), \ldots, x(0)(n)]^T \tag{12}$$

Step 5: Production of GM(1,1) Model:

This step is to determine the forecasted AGO data series of $x^{(1)}$, which is the solution at time instant k of (9):

$$\hat{x}^{(1)}(k+1) = (x_0 - \frac{u}{a})e^{-ak} + \frac{u}{a} \tag{13}$$

Step 6: Inverse accumulated generation operation (IAGO):

Because the grey forecasting model is formulated using the data of AGO rather than the original data, IAGO can be used to restore the forecasted values by (14) to obtain the forecasted data series $\hat{x}^{(0)}$

$$\hat{x}^{(0)}(k) = \hat{x}^{(1)}(k) - \hat{x}^{(1)}(k-1), \quad k = 2, 3, \ldots, n \tag{14}$$

Provided with the input data set of measured flicker severity level of $\Delta V10$ as the original data series for training, Fig. 2 illustrates the forecasting flowchart described above. In Fig. 2 the first three functional blocks are for the training and determining the two parameters of the GM(1,1) model. Then, the forecast of future $\Delta V(0)$ trend is performed through the last three blocks of operations.

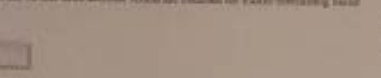

Fig. 2. Forecasting flowchart based on the grey model GM(1,1).

IV. Simulation Results

In this paper, the 161-kV system supplying a steel plant with a 45-ton arc EAF shown in Fig. 3 is used as the measured target, where measurements are taken at the EAF bus side. In addition, the flicker severity (i.e. voltage fluctuation assessment) index, $\Delta V10$, is calculated to identify if the index exceeds the allowable limit of 0.45% set by the local electric utility. A total number of 10080 measured data set of $\Delta V10$ over two weeks have been recorded. The flicker severity data set is divided into two parts to perform the flicker assessment in two modes: training and forecasting processes. Therefore, earlier measured data of $\Delta V10$ are used for training the proposed and two other methods under comparisons. Then, the forecast of future flicker values are performed after the three methods have been trained.

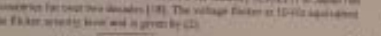

Fig. 3. EAF circuit diagram.

Fig. 4(a) shows the measured $\Delta V10$ caused by the arc EAF operation over three days for training the BPNN, RBFNN, and the proposed methods. In Fig. 4 (a), it is observed that the flicker severity limit of 0.45% is violated most of the time. Another one-week long measured data set for the forecast and comparison are shown in Fig. 4 (b). In Fig. 4(b), except those in the last two days, $\Delta V10$ patterns in the first five weekdays are similar. Figs. 4(c)-4(e) show the forecasted values of (b) by BPNN, RBFNN, and the proposed method, respectively. Figs. 4(f)-4(h) are show the corresponding forecasted errors of Figs. 4(c)-4(e), respectively. Table I lists the forecast errors in terms of mean absolute percentage error (MAPE) and root mean squared error (RMSE), as well as the solution, learning time for the three compared methods. By observing results shown in Fig. 4 and Table I, it is seen that the proposed method can accurately forecast $\Delta V10$ flicker severity level varied. Among the three forecasting methods, the proposed one can with the least errors and solution training time.

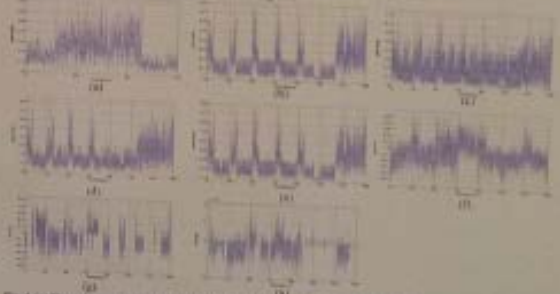

Fig. 4. (a) Three-day measured data of $\Delta V10$ for training; (b) 7-day measured data for forecast and comparison, (c) forecasted data of (b) by BPNN, (d) forecasted data of (b) by RBFNN, (e) forecasted data of (b) by the proposed method, (f) forecast errors of BPNN, (g) forecast errors of RBFNN, and (h) forecast errors of the proposed method.

Table I
Forecast Errors of Compared Methods and Needed Training Time

	MAPE	RMSE	CPU Time (sec)
BPNN	2.39e+01	8.47e+01	1.808
RBFNN	2.34e+01	7.32e+01	0.828
Proposed GM(1,1)	1.81e+01	6.09e+01	0.735

MAPE = $\frac{1}{n}\sum_{k=1}^{n}\left|\frac{\text{(actual value)}-\text{(forecasted value)}}{\text{(actual value)}}\right| \times 100\%$

RMSE = $\sqrt{\frac{1}{n}\sum_{k=1}^{n}[\text{(actual value)}-\text{(forecasted value)}]^2}$

V. Conclusion

In this paper, a grey model method for forecasting the flicker severity level of $\Delta V10$ associated with the arc EAF load has been proposed. Results obtained by the proposed method were compared with two commonly used neural network methods. It showed that the proposed grey predictor model gave an accurate forecast of the produced flicker level due to the operation of an arc EAF load.

Paper 55 **Feasibility Study Of SVC Installation In A Substation Network For Voltage Fluctuation Mitigation**

Feasibility Study of SVC Installation in a Substation Network for Voltage Fluctuation Mitigation

[illegible]

Abstract

The operation of electric arc furnaces (EAFs) with drastic and random voltage-current characteristics creates considerable power quality problems in the connected power network. Because of the nonlinear behaviors of the EAF loads during operations, serious voltage fluctuations have been observed at buses that connect the substation transformer and cause frequent operations of the on-load tap changer (OLTC) of the transformer, which may shorten the OLTC life and affect the voltage quality. To reduce the number of switching operations of the OLTC, it is necessary to adopt mitigation solutions. This paper presents a feasibility study of installing a static var compensator (SVC) in an actual substation network supplying two large EAF loads for mitigating the voltage fluctuation and the number of OLTC operations. The effectiveness of installing the SVC at selected buses and the corresponding size are then requested.

Index Terms — Electric Arc Furnace, Flicker, On-Load Tap Changer, Static Var Compensator

I. Introduction

Electric arc furnaces (EAFs) melt scrap metal with high temperature heat of arc between electrodes and metal. Due to the unstable characteristic of arc resistance during operations, the length of arc will change randomly according to the load conditions. Moreover, short and open circuits occur between electrodes while metal is continuously melting between electrodes. As a result, to discharge irregularly between electrodes causes reactive power fluctuates randomly and seriously, and large variations of current with low power factor create voltage fluctuation and power quality may be deteriorated.

Due to the nonlinear characteristic of EAF loads within a primary substation (PS) power network, serious voltage fluctuations have been observed at the bus connected to the substation transformers. The on-load tap changers (OLTC) of the transformer thus have frequently switched on and off, which may cause damages of transformers and also affect the quality of power supply. For mitigating such problems, it is necessary to estimate if it needs to install any flicker mitigation devices. Therefore, solutions are being searched and the installation of a SVC is considered to improve the power quality.

In the study, the authors analyze the power quality impact of severely EAF load variations on the feeder under the area where several steel-making customers are served by the PS. The authors use simulation techniques and accurate equipment models to test the actual study system and assess the effects of installing a SVC in the PS service network. To reduce the number of switched operations of the OLTC, this study adopts Matlab/Simulink and its built SVC model in SimPowerSystem toolbox for the simulation. Then, the OLTC operation behaviors before and after the SVC installation are observed. Finally, the effectiveness for voltage fluctuation due to EAFs and the size of the installed SVC are reported.

II. Modeling OLTC Regulation Transformer and Static Var Compensator

A. OLTC Regulation Transformer

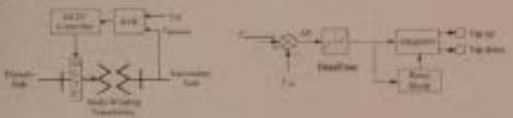

Fig.1 Configuration of the OLTC Regulation transformer

Fig.2 The control diagram of automatic voltage regulator (AVR)

B. Static Var Compensator (SVC)

Fig.3 Configuration of a typical SVC

III. Case Study

In the actual studied 161kV system, it includes *D* primary substation (PS), *E* distribution substation (DS), and three steel plants (*A*, *B*, and *C*). Plants *A* and *B* are on the same feeder (Feeder 1) and fed by *E* DS. Plant *C* is fed by *D* PS directly (Feeder 2). In plant *A*, there are one 90-ton DC EAF, one LF, one rolling mill and shunt capacitors for reactive power compensation. There are only two rolling mills in plant *B*. In plant *C*, there are one 43-ton AC EAF, one ladle furnace (LF), one SVC, and two rolling mills. The one-line diagram of studied system is shown in Fig. 5.

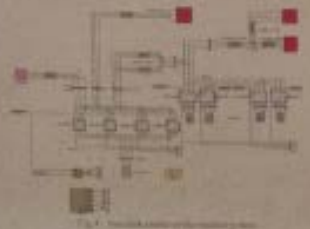

Fig.5 One-line diagram of the studied system

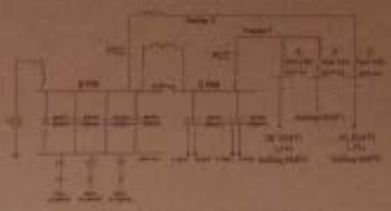

Fig.6 One-line diagram of the studied system

A. Without SVC

B. SVC Installation at Plant A

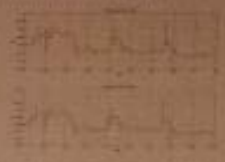

C. SVC Installation at D PS

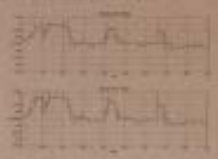

D. SVC Installation at E DS

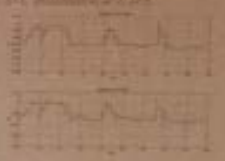

E. Observations

Table I lists the number of OLTC switched on and off at the primary side of the main transformer (MTR) at *D* PS and at the secondary sides of the two distribution transformers (DTR1 and DTR 2) at *E* DS. It shows that switched times of MTR and DTRs are 2, except of DTR 1 11.95kV. Though the number of OLTC operation times of DTR 1 increases from 0 to 2, the SVC installation still effectively mitigates the OLTC operation. As shown in Table III for Case 3, voltage fluctuation variation of *D* PS and *E* DS is 0.01 and 0.0164, respectively. In cases with SVC installation, the voltage fluctuation is effectively mitigated. In Table III, it shows that a smallest capacity of SVC can be achieved when it is placed at Plant *A*, because the SVC only needs to compensate local reactive power fluctuation, while the other two cases lead to more reactive power requirement of the SVC.

Table I: OLTC Operation at MTR and DTR

Installation Location	Number of OLTC Switch on and off				
	MTR 1:4	DTR 1 22.8kV	DTR 1 11.95kV	DTR 2 22.8kV	DTR 2 11.95kV
w/o SVC	2	2	0	2	2
SVC at *Plant A*	0	1	2	1	2
SVC at *D* PS	1	1	1	1	1
SVC at *E* DS	0	0	1	1	1

Table II: Flicker Voltage Variation Dependent Level

Installation Location	*D* PS	*E* DS
w/o SVC	0.0300	0.0364
SVC at *Plant A*	0.0150	0.0199
SVC at *D* PS	0.0100	0.0258
SVC at *E* DS	0.0162	0.0154

Table III: Location vs Capacity

Location	Capacity (MVAR)
Plant A	46.00
D PS	57.10
E DS	53.60

IV. Conclusion

This paper has presented a study of using SVC to mitigate voltage fluctuation and its impact on the OLTC through Matlab/Simulink modeling and simulation. Major contributions of this study are (1) modeling the OLTC regulation transformer with AVR are established and used to build the studied system, (2) different SVC installation locations are selected and simulations show that a SVC can effectively mitigate voltage fluctuation and reduce the number of OLTC switched on and off.

In addition to installing the SVC in the EAF load side (*Plant A*), the SVC also can be installed at the utility side to mitigate voltage fluctuation and enhance power quality of the supply system. However, the study shows that the best site to install is close to the EAF load, which not only mitigates the voltage fluctuation, but also improves the quality of the production. It requires a larger capacity of SVC and involves more cost when installing the compensator to the utility's PS power network.

CCU Power Quality Research Laboratory
Department of Electrical Engineering, National Chung Cheng University, Taiwan

Paper

62

Modeling And Simulation Of An AC Microgrid For Harmonics Study

Modeling and Simulation of an AC Microgrid for Harmonics Study

H.J. Su, G.W. Chang, Fellow, IEEE, S. Rueda, Senior Member, IEEE, and H.J. Liu

Abstract

The deployment of ac microgrids including distributed energy resources (DERs) can reduce the investment cost of building new fossil-fuel based power plants, facilitate the carbon-oxide reduction, provide reactive power compensation and frequency regulation, increasing spin reserve, and enhance the system stability. However, some undesired effects such as imbalance, voltage fluctuation, and harmonics accompanied with the operations of DERs and nonlinear loads, which may affect the power quality (PQ) within the microgrid system. This paper presents a simulation-based study of harmonics impact within an ac microgrid and the effectiveness of the mitigation solutions. Results obtained illustrate that potential harmonic problems are identified and the harmonics mitigating solutions can be used for the planning of a microgrid deployment and its PQ assessments.

Index Terms — AC microgrid, Power Quality, Frequency Scan, Active Power Filter, Passive Harmonic Filter.

I. Introduction

Due to the characteristics of distributed energy resources (DERs), modern power systems have faced significant operation transformations. For instance, the power flow is changed from one-directional to bi-directional. Also, active distributed systems have flexible and smart control systems to obtain clean energy from renewable sources. Consequently, distribution systems have turned into smart grids or localized microgrids. Microgrids are hybrid systems which may consist of wind generators, fuel cells, photovoltaics (PV) cells, microturbines, and loads, which provide the solution to supply premium power to remote or specific areas.

Though many advantages are provided by deploying microgrids, there are also some issues to be addressed on the microgrid such as protection coordination, voltage regulation, and power quality including imbalance, harmonics, and flicker. For the microgrid, significant voltage fluctuations are caused by variations of active and reactive power of distributed energy resources (DERs) and may affect the grid stability and reliability. In addition, harmonic currents produced by DERs and nonlinear loads may interact with system impedance and cause voltage distortion. Supplying premium power and maintaining good power quality has become of great concern for operating microgrids.

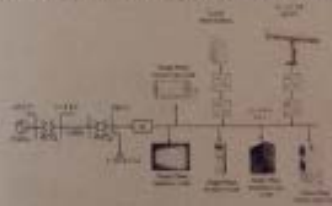

Fig. 1. A typical configuration of the ac microgrid.

II. Microgrid System Response to Harmonics

The h-th order of harmonic voltage at each grid bus then can be expressed by (1) or (2)

$$V_h = Z_h \cdot I_h \qquad (1)$$

$$I_h = Y_h \cdot V_h \qquad (2)$$

where V_h is harmonic voltage source, I_h is measured or estimated harmonic current source, and Z_h and Y_h are harmonic impedance and admittance matrices, respectively.

Equations (1) and (2) used in harmonic analysis are called harmonic (current, voltage) coupling. This approach is usually combined with fundamental power flow analysis. With system harmonic impedance and harmonic current injected by considered non-linear loads, individual and total harmonic voltage distortion (THD) can be determined.

In (1), it can be found that system harmonic impedance plays a very role in the system harmonic response. Resonant frequencies of the grid can be identified through frequency scan. In a microgrid system, the main resonant source is installations of capacitor banks which are used to correct power factor or to regulate voltage.

Commonly used mitigation of harmonic resonance includes passive harmonic filter (PHF) or active power filter (APF) installation. PHFs is to prevent particular orders of harmonic currents from flowing into the system, and it can lower voltage or current sensitivity of some frequency to suppress harmonic effects, to limit harmonic distortion, and to ensure power quality pollution and risk of damaging equipments. Single-tuned filters are the most often used approach to shunt low orders of harmonic currents. The APFs generate compensative current with equal amplitude and opposite polarity to eliminate harmonic current in the system. APFs provide multiple features such as harmonic filtering, reactive power compensation, power factor correction, and load balance.

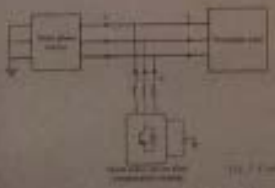

Fig. 2 Configuration of a three-phase three-wire...

III. System Modeling

A. Modeling Non-linear Loads

For modeling the non-linear loads, the harmonic injection approach mentioned in the previous section is used. The current waveforms of non-linear loads can be determined with actual measured current waveforms through fast Fourier transform (FFT). The spectra include magnitudes and phase angles which can be used to represent harmonic current injection models.

B. Modeling Photovoltaic, Storage and Fly-wheel Systems

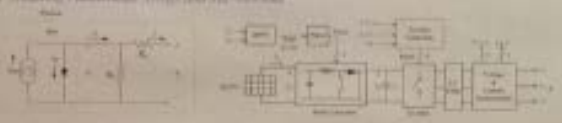

Fig. 3 The equivalent single-phase PV module and schematic diagram of the PV system.

Fig. 4. The schematic diagram of the fly-wheel energy generation system.

IV. Case Study

Fig. 5. The test system diagram for the microgrid.

Fig. 6. Frequency scan of a microgrid at bus 1.

Fig. 7. Voltage and current waveforms at bus 1.

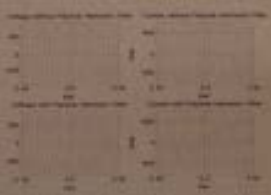

Fig. 8. Current and voltage waveforms at the utility source terminal.

Fig. 9. Harmonic spectrum of the current at the utility source terminal.

Table 1 Comparisons of THD at bus 1 and bus 2 with/without the mitigation devices

	THD	PHF	APF
THD, at load side	15.95%	-	4.54%
THD, at the 1[1] node	5.33%	0.16%	0.64%
THD, at the 1[2] node	15.29%	-	1.46%
THD, at LV side of the transformer	7.19%	0.46%	-

V. Conclusion

This paper has presented a study of harmonics impact of an ac microgrid for the initial phase of deployment. The detailed models of the microgrid components were well modeled and simulations were performed to observe the harmonic impact to the system and the mechanisms of the harmonics mitigating solutions. It is expected that the modeling and simulation method can be used and extended to include more DERs for next phase of microgrid deployment and associated power quality study.

VI. Acknowledgements

The authors would like to thank the Institute of Nuclear Energy Research, Taiwan, R.O.C., for the financial support of this microgrid deployment project.

附件二


港燈
HK Electric
電能質量中心
POWER QUALITY CENTRE